JHEP

Published for SISSA by Springer

Received: February 26, 2016
Accepted: April 6, 2016
Published: May 2, 2016

The two-loop symbol of all multi-Regge regions

Till Bargheer,[a] **Georgios Papathanasiou**[b] **and Volker Schomerus**[a]

[a] *DESY Theory Group, DESY Hamburg, Notkestraße 85, Hamburg, D-22607 Germany*

[b] *LAC National Accelerator Laboratory, Stanford University, Stanford, CA, 94309 U.S.A.*

E-mail: till.bargheer@desy.de, georgios@slac.stanford.edu, volker.schomerus@desy.de

Abstract: We study the symbol of the two-loop n-gluon MHV amplitude for all Mandelstam regions in multi-Regge kinematics in $\mathcal{N} = 4$ super Yang-Mills theory. While the number of distinct Mandelstam regions grows exponentially with n, the increase of independent symbols turns out to be merely quadratic. We uncover how to construct the symbols for any number of external gluons from just two building blocks which are naturally associated with the six- and seven-gluon amplitude, respectively. The second building block is entirely new, and in addition to its symbol, we also construct a prototype function that correctly reproduces all terms of maximal functional transcendentality.

Keywords: Scattering Amplitudes, Supersymmetric gauge theory, 1/N Expansion, Extended Supersymmetry

ArXiv ePrint: 1512.07620

doi:10.1007/JHEP05(2016)012

JHEP05(2016)012

Contents

JHEP05(2016)012

1 Introduction

Constructing the S-matrix of a 4D gauge theory, even in the planar limit, is one of the central challenges of theoretical physics. In the case of $\mathcal{N} = 4$ supersymmetric Yang-Mills (SYM) theory, dual conformal symmetry [1, 2] uniquely fixes the form of scattering amplitudes of up to 5 external gluons to coincide with the BDS ansatz [3]. But it allows for an additional finite part that can depend on $3n - 15$ conformal cross ratios for amplitudes with $n \geq 6$ gluons. Impressive progress towards the determination of the latter quantity has been made, in particular for $n = 6$ external gluons. In this case, there exists an all-loop formula which determines the remainder function for general kinematics [4]. A number of complementary approaches paved the way for this important result. These included perturbative studies in special kinematic regions, such as the collinear and the Regge limit, see [5–7] and [8–10] for early contributions. Their findings provided essential boundary conditions into the amplitude bootstrap for fixed-order calculations in general kinematics that was initiated in [11] (see also [12] for a recent overview and more references). In a series of papers [4, 13–17], Basso et al. then developed the non-perturbative Wilson loop OPE, and showed that it could accommodate all previous results on hexagon amplitudes and even correctly interpolate to strong coupling where string theory takes over [18–22].

While some partial results are known in particular for $n = 7$, see e.g. [23–27] and references therein, the scattering problem of $\mathcal{N} = 4$ SYM theory with more than six gluons has not been solved. In pushing the entire program to higher numbers of external gluons and uncovering universal patterns, the multi-Regge limit of high-energy gluon scattering is expected to play an important role. Similar to the Wilson loop OPE, the expansion around

multi-Regge kinematics is based on elementary building blocks, such as BFKL eigenvalues, impact factors and production vertices. These are subject to powerful constraints from integrability which have been partially worked out, see e.g. [28]. In addition, the multi-Regge limit was shown [29] to correspond to the infrared limit of the auxiliary one-dimensional integrable system that controls the strongly coupled theory [20]. In this regime, the quantum fluctuations of the auxiliary system are suppressed, which turns the original system of coupled non-linear integral equations into much simpler algebraic equations for Bethe roots.

Turning to the amplitude bootstrap, we recall that it relies on the observation that L-loop amplitudes of certain helicity are expressed in terms of multiple polylogarithm functions [30] of transcendental weight $2L$ (see [31] for a review). This is backed by the "dlog" representation of the all-loop integrand [32], as well as the perturbative analysis of the OPE expansion [33–35]. However, except for six and seven particles [36], to date we know of no principle that would motivate from which set of "letters" (or "alphabet") these multiple polylogarithms can draw their arguments. The multi-Regge limit could serve as a stepping stone in this direction, since the kinematical dependence simplifies considerably, and the experience from the six-gluon analysis suggests that amplitudes inherit special analytic properties in this limit [37]. These properties are also expected to make the evaluation of the integral formulas describing the amplitude in the limit much simpler than the ones arising in the OPE approach around collinear kinematics, where the question of resummation at weak and strong coupling represents a formidable task [15, 34, 38, 39].

With these goals in mind, we will focus on the multi-Regge limit of the simplest, Maximally Helicity Violating (MHV) n-gluon amplitudes with all but two of the helicities being the same. For these amplitudes, the finite part not fixed by dual conformal symmetry is a single *remainder function* R_n. Although the multi-Regge limit of the latter vanishes in the Euclidean region where all Mandelstam invariants are spacelike [40, 41], it possesses a rich set of branch cuts. Exploring the branch structure through analytic continuation in the Mandelstam invariants leads to various Mandelstam regions with non-trivial multi-Regge limit. The number of different regions increases exponentially with the particle number, hence it is natural to ask for the simplest subset of regions that contains all the independent "boundary data" to be used for constructing the amplitude in general kinematics.

In this note we consider the $2 \to (n-2)$ multi-Regge limit in 2^{n-4} different Mandelstam regions, which are reached by analytic continuation in the momenta of any combination of $(n-4)$ adjacent external particles from positive energy (in the Euclidean region) to negative energy. Our starting point is the known two-loop n-point MHV symbol [42]. Symbols [31, 43–45] capture the most complicated part of the amplitude with the highest *functional* transcendental weight in a way that trivializes all identities among (multiple) polylogarithms. The investigation of the multi-Regge limit of two-loop symbol was initiated in [46], restricted to the leading term in the multi-Regge limit (leading logarithmic approximation, or LLA), and for a single Mandelstam region. Our analysis extends both aspects: we consider all 2^{n-4} Mandelstam regions, and we include the first subleading term in the multi-Regge limit (NLLA). As results, we shall find that *(i)* all independent information is contained in a subset of only $(n-4)(n-5)/2$ regions and *(ii)* in all regions

JHEP05(2016)012

the multi-Regge limit of the symbol decomposes into two basic building blocks f and g, naturally associated to the $n = 6$ and $n = 7$ symbols, respectively. The first building block f was already discussed in [9, 46] to LLA, and here we identify it to NLLA. The second object g, which receives contributions only from NLLA, is entirely new. Apart from spelling it out explicitly, we also find a functional representative for it, belonging to the class of two-dimensional harmonic polylogarithms (2dHPLs) [47]. We complete the construction through a prescription for how to build the two-loop symbol in the multi-Regge limit of 2^{n-4} Mandelstam regions for any number of external gluons from the building blocks f and g.

This article is organized as follows. In section 2 we briefly review some basic facts about iterated integrals, symbols and their discontinuities. We apply these in section 3 to obtain the form of the two-loop n-point symbol in the different Mandelstam regions, after also discussing how these can be reached by analytically continuing the kinematical invariants. In section 4 we take the multi-Regge limit of the symbol, and show how the answer in any region may be reconstructed from the simplest regions in which only a single branch cut contributes to the multi-Regge limit. One of the main results of the paper, the decomposition of the symbol into the two building blocks for these regions, is the subject of section 5. Section 6 deals with the uplift of the newly found seven-gluon building block to a function, whereby we uniquely fix the maximal transcendental part, and further constrain the possible terms of lower transcendentality by symmetry. Section 7 contains our conclusions. In appendix A, we present a particular parametrization of the kinematics in terms of momentum twistors that we found very useful for our analysis.

Computer-readable files with our results accompany our article on the `arXiv`. This data constitutes an important step towards determining the new quantity appearing in the Balitsky-Fadin-Kuraev-Lipatov (BFKL) approach for R_7 known as the central emission vertex, that so far has only been computed to LLA [23, 26]. Furthermore, the decomposition we have discovered is suggestive of a factorization structure that may impose new constraints on the analogous BFKL quantities also appearing at higher points.

2 Symbols and discontinuities

Let us consider the $(3n-15)$-dimensional space $\mathcal{X}$ of independent dual conformal invariant cross ratios for an n-gluon scattering process, and a curve $\gamma : [0,1] \to \mathcal{X}$ in the space of kinematic invariants. It starts at the base point $\gamma(0) \in \mathcal{X}$ and can run to any point $\mathrm{x} = \gamma(1) \in \mathcal{X}$. At two loops, the remainder function is a sum of iterated integrals [48] of the form

$$R(\mathrm{x}) \sim \int_{0 \le t_1 \le \cdots \le t_4 \le 1} \mathrm{dlog}(X_{a_1}(t_1)) \ldots \mathrm{dlog}(X_{a_4}(t_4)) \,, \tag{2.1}$$

where X_a is some set of functions on $\mathcal{X}$, indexed by some finite index set, i.e. $a = 1, \ldots, \varpi$, which depend on the parameter $t \in [0,1]$ through the curve γ. In order to keep notations simple we have only displayed a single summand. The symbol $\sim$ should remind us of the fact that the true remainder function R is composed from a finite sum of such

JHEP05(2016)012

integral contributions. All of them contain four integrations, i.e. they possess the same transcendentality degree, or weight.

In order for the integral to be well-defined, we should avoid curves γ which pass through the set $\mathcal{Z}$ of zeros and singularities of X_a. Consequently, $R(\mathrm{x})$ is only defined for $\mathrm{x} \in \mathcal{Y} \equiv \mathcal{X} \setminus \mathcal{Z}$. There exists an integrability condition, which insures that an iterated integral depends only on the base point $\gamma(0)$ and the homotopy class $[\gamma]$ of γ in $\mathcal{Y}$ [48]. Provided the integrability condition holds, and given a base point $\gamma(0)$, the integral R defines a multivalued function on $\mathcal{Y}$. It has branch cuts B_ν which end at the zeros and singularities of the entries X_a. The discontinuities Disc_ν along the branch cuts are given by

$$\mathrm{Disc}_\nu(R(\mathrm{x})) \sim \sum_{j=1}^{4} \int\limits_{0\leq s_1\leq\cdots\leq s_j\leq 1} \mathrm{dlog}(X_{a_1}(s_1))\ldots\mathrm{dlog}(X_{a_j}(s_j)) \int\limits_{0\leq t_{j+1}\leq\cdots\leq t_4\leq 1} \mathrm{dlog}(X_{a_{j+1}}(t_{j+1}))\ldots\mathrm{dlog}(X_{a_4}(t_4))\,. \quad (2.2)$$

In this expression, the parameters t_i are mapped into the space $\mathcal{Y}$ of kinematic invariants through the curve γ, as before, while s_i are sent to $\mathcal{Y}$ through a closed curve $\eta_\nu = \eta_\nu(s)$ which starts and ends at $\gamma(0)$, winds around the branch point B_ν once, and avoids winding around all other B_μ, $\nu \neq \mu$. Consequently, the integral on the left in the above equation evaluates to a number, i.e. it does not depend on the endpoint x of the curve γ. All dependence on x comes in through the iterated integrals on the right. In order to derive this expression, one moves the base point $\gamma(0)$ along the closed curve η_ν. The iterated integral along the concatenation $\gamma \circ \eta$ decomposes into a sum of products of iterated integrals of lower functional transcendentality. By definition, the discontinuity is the difference between the integral for $\gamma \circ \eta$ and the original γ. It is a linear combinations of iterated integrals of functional transcendentality degree less or equal to three.

The symbol $\mathrm{S}[R]$ is a linear map on the space of iterated integrals which is defined such that [43]

$$S[R(\mathrm{x})] \sim (X_{a_1} \otimes \cdots \otimes X_{a_4})\ . \quad (2.3)$$

Note that the symbol forgets all information encoded in the choice of the base point and path. Hence, it determines the original iterated integral R only up to certain functions of lower transcendentality. On the other hand, it knows about the endpoints of branch cuts and allows to determine the symbol of the corresponding discontinuities,

$$S[\mathrm{Disc}_\nu(R(\mathrm{x}))] \sim \left[\oint_{\eta_\nu} \mathrm{dlog}(X_{a_1})\right]\ (X_{a_2} \otimes \cdots \otimes X_{a_4})\ , \quad (2.4)$$

From the right hand side, we can reconstruct the discontinuity up to certain functions of transcendentality degree less or equal to two.

Before we conclude this section, let us make one more comment. The discontinuities across branch cuts provide a representation of the homotopy group $\pi_1(\mathcal{Y})$. On the other hand, commutators of elements in the homotopy group are related to double discontinuities, and hence these are expressed through iterated integrals of transcendentality at most two. Such integrals do not show up in a symbol of length three and hence we will be able to safely ignore the difference between homotopy and homology in the following analysis.

JHEP05(2016)012

3 Mandelstam regions and cuts

A relatively simple expression for the two-loop remainder functions has been found for $n = 6$ in [44]. The two-loop remainder function was also determined for $n = 7$ in [24], but the expressions are quite complex already. On the other hand, the symbol of the two-loop remainder function is actually known for any number n of gluons [42]. As we have just recalled, this symbol determines the finite remainder $R_n^{(2)}$ up to functions of transcendentality at most three. Our goal is to analyze this symbol, and in particular the symbol of its discontinuities, in the multi-Regge limit.

As we reviewed above, to leading transcendental order the remainder function has branch cuts that end at the zeros and infinities of those functions X_a that appear as a first entry of the symbol. The positions of these branch cuts are dictated by unitarity to coincide with thresholds where an intermediate particle goes on shell. For planar massless theories, this can only happen when a sum of cyclically adjacent external momenta becomes null [7]. Since dual conformal invariance additionally constrains the remainder function to only depend on conformal invariant combinations of Mandelstam invariants, from these considerations we deduce that the first entries of the symbol can only be cross ratios of the form

$$U_{ij} = \frac{x_{i+1,j}^2 x_{i,j+1}^2}{x_{ij}^2 x_{i+1,j+1}^2} \,. \tag{3.1}$$

These are defined for $i, j = 1, 2, \ldots n$ and $3 \leq |i - j| \leq n - 2$ in terms of the distances

$$x_{ij}^2 = (x_i - x_j)^2 \tag{3.2}$$

between the cusps x_i of the usual light-like polygon that encodes the kinematics of the scattering event through $p_i = x_i - x_{i-1}$. Our conventions concerning the enumeration of gluons are shown in figure 1. The black dots on the right hand side depict the cusps. Counting the different possibilities in eq. (3.1) we see that we can have a total of $n(n-5)/2$ distinct cross ratios. While $(n-4)(n-5)/2$ of them are given by the cross ratios

$$u_{ij} = U_{ij} \qquad \text{with} \quad i = 2, \ldots, n-4, \quad j = i+3, \ldots, n-1 \,, \tag{3.3}$$

it turns out convenient to use $2(n-5)$ products and quotients of the remaining cross ratios U_{1j} and $U_{j-1,n}$,

$$\tilde{u}_j := U_{1j} U_{j-1,n}^{-1} \,, \qquad \varepsilon_j := U_{1j} U_{j-1,n} \tag{3.4}$$

where $j = 4, \ldots, n-2$. Of course, the usual rules of the symbol calculus allow to pass easily from $\tilde{u}_j$ and ε_j to the more conventional first entries U_{1j} and $U_{j-1,n}$.

Our goal is to analyze the discontinuities along the cuts that end at points where one of the kinematic invariants u, $\tilde{u}$, or ε vanish. We will restrict attention to those discontinuities that are picked up while we continue the kinematic invariants into so-called Mandelstam regions, i.e. into regions in which some of the s-like variables s_i are negative, see figure 1. These regions are reached by continuing the energies p_j^0 of outgoing particles with indices $j \in I \subset \{4, \ldots, n-1\}$ to negative values. The choice of the subset I labels the different Mandelstam regions.

JHEP05(2016)012

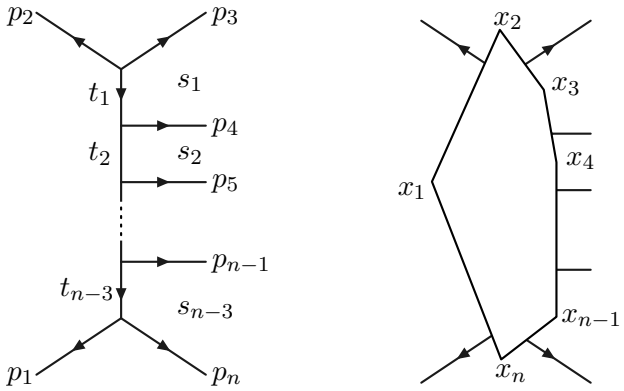

Figure 1. Kinematics of the scattering process $2 \to n-2$. On the right-hand side we show a graphical representation of the dual variables x_i.

To each such Mandelstam region I we associate an n-component object $\rho^I = (\varrho_j^I)$ such that

$$\varrho_j^I = \begin{cases} -1 & \text{if } j \in I \\ 0 & \text{if } j \in \{1 \equiv n+1, 2\} \\ +1 & \text{otherwise.} \end{cases} \tag{3.5}$$

In order to reach a region $\rho = (\varrho_a)$, the curve in the space of kinematic invariants has to wind around the endpoints of some of our branch cuts. For the points $u_{ij} = 0$, the winding numbers are [27]

$$n_{ij}(\rho) = \frac{1}{4}(\varrho_{i+1} - \varrho_{i+2})(\varrho_{j+1} - \varrho_j) \ . \tag{3.6}$$

From the formulas in [27] one can also conclude that the points $\varepsilon_j = 0$ possess trivial winding for all Mandelstam regions ρ while for $\tilde{u}_j$ one finds

$$n_j(\rho) = \frac{1}{2}(\varrho_j - \varrho_{j+1}) \ . \tag{3.7}$$

With these basics set up, our next aim is to establish a number of relations between the winding numbers for different Mandelstam regions ρ. The simplest winding numbers appear for the Mandelstam regions $\rho^{[k,l]}$ that are associated with sets $I = [k,l] = \{k, k+1, \ldots, l-1, l\}$ with $4 \le k \le l \le n-1$. For these regions, the winding numbers around the branch points in u_{ij} are

$$n_{ij}(\rho^{[k,l]}) = \delta_{i,k-2}\delta_{j,l} \ . \tag{3.8}$$

while for the branch points in $\tilde{u}_j$ one finds

$$n_j(\rho^{[k,l]}) = \delta_{j,k-1} - \delta_{j,l} \ . \tag{3.9}$$

Note that any such region with $k \neq l$ is associated with a unique cross ratio $u_{k-2,l}$ that winds during the continuation into the Mandelstam region $\rho^{[k,l]}$. Let us point out that the above formulas can also be applied to regions $\rho^k = \rho^{\{k\}}$ associated with a single sign flip by setting $k = l$. In this case the winding numbers n_{ij} vanish, while $n_j(\rho^k) = \delta_{j,k-1} - \delta_{j,k}$.

JHEP05(2016)012

The winding numbers n_{ij} around the branch points $u_{ij} = 0$ obey two interesting relations that will become important later on. It is not difficult to see that

$$n_{ij}(\rho^I) = \sum_{\{k,l\}\subset I} n_{ij}(\rho^{\{k,l\}}) \tag{3.10}$$

and

$$n_{ij}(\rho^{\{k,l\}}) = n_{ij}(\rho^{[k,l]}) - n_{ij}(\rho^{[k+1,l]}) - n_{ij}(\rho^{[k,l-1]}) + n_{ij}(\rho^{[k+1,l-1]}) \ . \tag{3.11}$$

Let us stress that these relations are not to be read as equalities in homology, since they do not hold for the winding numbers n_j. Given the symbol for the 2-loop n-gluon remainder function,

$$\mathrm{S}[R] = \sum u_{ij} \otimes S_{ij} + \sum \left(\tilde{u}_j \otimes S_j + \varepsilon_j \otimes \tilde{S}_j \right) \tag{3.12}$$

we can associate a symbol of length three

$$\mathrm{S}[R]_\rho \equiv -2\pi i \sum n_{ij}(\rho) S_{ij} - 2\pi i \sum n_j(\rho) S_j \ . \tag{3.13}$$

to every Mandelstam region. Here we have used that none of our curves winds around the branch points in $\varepsilon_j = 0$. Like the original symbol, the symbols S_{ij} and S_j of the cut contributions are a bit complicated. What matters to us is that they can be worked out from the formula for $\mathrm{S}[R]$.

4 Multi-Regge limit and relations

The multi-Regge limit is a scaling limit in which the pairwise subenergies $s_{j-3} = (p_{j-1}+p_j)^2$ for $j = 4, \ldots, n-1$ are sent to infinity while keeping the t-like variables in figure 1 along the so-called Toller angles finite, see [29] for details. One can show that this limiting procedure is equivalent to sending

$$\varepsilon_j \to 0 \tag{4.1}$$

while keeping $\tilde{u}_j$ and $(1 - u_{j-2,j+1})^2 \varepsilon_j^{-1}$ finite for $j = 4, \ldots, n-2$. The entries X of the symbol are functions of the kinematic invariants. For each of them there exists a unique monomial X^{MRL} in the variables ε_j such that

$$\lim_{|\varepsilon_j|\to 0} X/X^{\mathrm{MRL}} = 1 \ . \tag{4.2}$$

The coefficient factor in X^{MRL} still depends on $2n-10$ kinematic invariants $w_j, \bar{w}_j$, see below.

In order to compute the multi-Regge limit of the symbol of the discontinuities, we parametrize the entries in terms of a natural set of $3(n-5)$ variables similar to the ones used in the computation of the OPE for polygon Wilson loops [5–7, 13, 49], see appendix A. For the following general discussion, it will be sufficient to know the multi-Regge limit of the first entry. This is given by [29]

$$u_{ij}^{\mathrm{MRL}} = 1, \qquad \tilde{u}_j^{\mathrm{MRL}} = w_j \bar{w}_j, \qquad \varepsilon_j^{\mathrm{MRL}} = \varepsilon_j \ . \tag{4.3}$$

JHEP05(2016)012

Note that we have introduced $w_a\bar{w}_a, a = 1, \ldots, n-5$ through the multi-Regge limit of $\tilde{u}_j$. In order to determine the complex variables w_a and $\bar{w}_a$ themselves, rather than their products only, we need to consider further combinations of kinematic invariants, namely

$$\left[(1-u_{j-2,j+1})U^{-1}_{j-1,n}\right]^{\text{MRL}} = (1+w_j)(1+\bar{w}_j)\ . \tag{4.4}$$

Now that we have defined the multi-Regge limit, let us return to the remainder function and determine the multi-Regge limit of its symbol. Let us recall that the remainder function R_n on the Euclidean sheet, where all the $s_i > 0$, vanishes in the multi-Regge limit. This implies that also its symbol must vanish. If we apply our construction of S^{MRL} to the symbol (3.12) we find that

$$0 = \text{S}[R]^{\text{MRL}} = \sum \left(w_j\bar{w}_j \otimes S^{\text{MRL}}_j + \varepsilon_j \otimes \tilde{S}^{\text{MRL}}_j \right). \tag{4.5}$$

Here we have dropped all terms containing S_{ij} since $1 \otimes S^{\text{MRL}}_{ij} \equiv 0$. From the previous equation we conclude that $S^{\text{MRL}}_j = 0 = \tilde{S}^{\text{MRL}}_j$. If we insert this into our expressions (3.13) for the cut contributions we obtain[1]

$$\text{S}[R]^{\text{MRL}}_{\rho} = -2\pi i \sum n_{ij}(\rho) S^{\text{MRL}}_{ij}\ . \tag{4.6}$$

Before we draw further conclusions from here, let us comment that our result $S^{\text{MRL}}_j = 0$ is fully consistent with the well-known fact that there are no non-trivial cut contributions to the continuation into Mandelstam regions ρ^k associated with a single sign flip [50] (reviewed in [26]). As we saw before, while we continue into these Mandelstam regions, only the variables $\tilde{u}_j$ with $j = k, k-1$ wind around $\tilde{u}_j = 0$. In order for the cut contribution to cancel we must have $S^{\text{MRL}}_k = S^{\text{MRL}}_{k-1}$, i.e. all these symbols must be identical, which is consistent with the stronger statement $S^{\text{MRL}}_j = 0$ we derived above.

The result (4.6) says that the multi-Regge limit of the symbol for any region ρ only depends on the winding numbers n_{ij}. Consequently, the two relations (3.10) and (3.11) translate into relations for the symbol

$$\text{S}[R_n]^{\text{MRL}}_I = \sum_{\{k,l\}\subset I} \text{S}[R_n]^{\text{MRL}}_{\{k,l\}}\,. \tag{4.7}$$

and

$$\text{S}[R_n]^{\text{MRL}}_{\{k,l\}} = \text{S}[R_n]^{\text{MRL}}_{[k,l]} - \text{S}[R_n]^{\text{MRL}}_{[k,l-1]} - \text{S}[R_n]^{\text{MRL}}_{[k+1,l]} + \text{S}[R_n]^{\text{MRL}}_{[k+1,l-1]}\,. \tag{4.8}$$

These relations imply that we can reconstruct the symbol of all Mandelstam regions from the symbol of those $(n-4)(n-5)/2$ regions that are associated with (any number of) adjacent flips. Let us note that the relations in this and the preceding section are independent of the loop order, as long as we restrict to the contributions of maximal functional transcendentality. In the case of $n = 7$ external gluons, such relations between different multi-Regge regions were first explored in [26], see e.g. formulas (6.1)–(6.8) in the concluding section of that paper. The last formula of that list, for instance, correspondents to our equation (4.8) with $n = 7, k = 4$ and $l = 6$, keeping in mind that $\text{S}[R_n]^{\text{MRL}}_{[5,5]}$ vanishes. Our results extend such relations to arbitary numbers of gluons, at least for the terms of maximal functional transcendentality which are captured by the symbol.

[1] We thank James Drummond for discussions around this point.

JHEP05(2016)012

5 Building blocks of the symbol

Having found all these relations between the Mandelstam regions we want to finally describe the multi-Regge limit of the symbol for the regions $\rho^{[k,l]}$, in which the adjacent particles $k, k+1, \ldots, l$ have their energy signs flipped. From these symbols, we will be able to construct the symbols in all other regions $\rho = \rho^I$ as linear combinations, following the relations (4.7) and (4.8). For the regions $\rho^{[k,l]}$, we find

$$\frac{\mathrm{S}[R_n]^{\mathrm{MRL}}_{[k,l]}}{2\pi i} = \sum_{i=k}^{l-1} \Big(f(v_i) \log \varepsilon_i + \tilde{f}(v_i) \Big) + \sum_{i=k}^{l-2} g(v_i, v_{i+1}) \,, \tag{5.1}$$

where the terms in the first sum are obtained from the two-loop remainder function for $n = 6$ external gluons as

$$f(v_4) \log \varepsilon_4 + \tilde{f}(v_4) = \frac{\mathrm{S}[R_6]^{\mathrm{MRL}}_{[4,5]}}{2\pi i} \,, \tag{5.2}$$

and the symbol g that appears in the second sum is related to the two-loop remainder function for $n = 7$ external gluons through

$$g(v_4, v_5) = \frac{\mathrm{S}[R_7]^{\mathrm{MRL}}_{[4,6]}}{2\pi i} - \sum_{i=4,5} \Big(f(v_i) \log \varepsilon_i + \tilde{f}(v_i) \Big) \,. \tag{5.3}$$

In order to recycle this data from $n = 6$ and $n = 7$ for the symbol of the two-loop remainder function for any number n of external gluons, as described in equation (5.1), we introduced a new set of variables $v_i, i = k, \ldots, l-1$ that are related to the kinematic variables w_i by

$$w_j = \frac{(v_j - v_{j-1})(1 + v_{j+1})}{(v_{j+1} - v_j)(1 + v_{j-1})} \,, \qquad j \in \{k, \ldots, l-1\} \,, \tag{5.4}$$

with the boundary conditions $v_{k-1} = 0$, $v_l = \infty$. Let us stress that this map between the v_i and w_j depends on the Mandelstam region $\rho^{[k,l]}$ we consider, and let us mention a few examples for concreteness: in the $\rho^{[4,5]}$ region relevant for R_6 in (5.2) we simply have $w_4 \equiv w = v_4$, whereas in the $\rho^{[4,6]}$ region relevant for R_7 in (5.3) we have

$$w_4 = \frac{v_4 \, (1 + v_5)}{v_5 - v_4} \,, \qquad w_5 = \frac{v_5 - v_4}{1 + v_4} \,. \tag{5.5}$$

For completeness, the inversion of (5.4) reads

$$v_j = \frac{(1 + (1 + (\ldots (1 + w_k) w_{k+1}) \ldots) w_{j-1}) w_j w_{j+1} \ldots w_{l-1}}{1 + (1 + (\ldots (1 + w_{j+1}) w_{j+2}) \ldots) w_{l-1}} \,, \qquad j \in \{k, \ldots, l-1\} \,. \tag{5.6}$$

In order to fully describe the symbol for all Mandelstam regions, it remains to spell out formulas for the symbols f, $\tilde{f}$ and g. The expression for f is known [46], it reads

$$f(w) = \frac{1}{2} \left((1+w)(1+\bar{w}) \otimes \frac{(1+w)(1+\bar{w})}{w\bar{w}} \right) + \frac{1}{2} \left(\frac{(1+w)(1+\bar{w})}{w\bar{w}} \otimes (1+w)(1+\bar{w}) \right) \,. \tag{5.7}$$

JHEP05(2016)012

Similar expressions for $\tilde{f}$ and g can be found in the MATHEMATICA file `SR2MRL.m` accompanying this publication. Let us only mention that the letters of the symbol $g(-1/y, -x)$ are x, y, $(1-x)$, $(1-y)$, $(1-xy)$, and their complex conjugates. Leaving the complex conjugate letters aside for a moment, functions with this five-letter symbol alphabet belong to the class of 2-dimensional harmonic polylogarithms (2dHPLs) [47], and in particular to the same subset which was found to describe the contribution of all single-particle gluonic bound states in the OPE expansion of the six-point remainder function [35].

Before concluding this section, let us summarize how the result (5.1)–(5.4) was obtained. Our starting point, the n-point two-loop MHV symbol in general kinematics has been derived in [42], by extending the duality between MHV amplitudes and bosonic Wilson loops [18, 51, 52] to the supersymmetric case. The result, which is also contained in a MATHEMATICA file accompanying the `arXiv` submission of the aforementioned article, encodes the kinematical dependence through momentum twistors Z_i, and in particular their scalar products, known as four-brackets,

$$\langle Z_i Z_j Z_k Z_\ell \rangle \equiv \epsilon_{abcd} Z_i^a Z_j^b Z_k^c Z_\ell^d \equiv \langle ijkl \rangle \,, \tag{5.8}$$

and their bilinears

$$\langle ij(abc) \cap (def) \rangle \equiv \langle iabc \rangle \langle jdef \rangle - \langle jabc \rangle \langle idef \rangle \,, \tag{5.9}$$

$$\langle i(ab)(cd)(ef) \rangle \equiv \langle aicd \rangle \langle bief \rangle - \langle aief \rangle \langle bicd \rangle \,. \tag{5.10}$$

We evaluate these expressions in any convenient set of variables, for example the one described in appendix A, and Taylor expand the symbol entries around the multi-Regge limit (in this case $T_i \to 0$, with S_i/T_i fixed, for $i = 1, \ldots, n-5$), keeping only the first term in the expansion of each entry. We may then trade the expansion parameters for the kinematic parameters ε_i we defined in eq. (3.4) that also become small in multi-Regge kinematics, see eq. (4.1), and the surviving $2(n-5)$ kinematical parameters for the $w_i, \bar{w}_i$ variables defined in eqs. (4.3), (4.4). After that, we factor the symbol entries and then expand the factors according to the symbol property,

$$A \otimes (X_a X_b) \otimes B = A \otimes X_a \otimes B + A \otimes X_b \otimes B \,, \tag{5.11}$$

which in particular also implies

$$A \otimes X^m \otimes B = m \, (A \otimes X \otimes B) \,. \tag{5.12}$$

These stem from the definition (2.1), (2.3), where it is evident that the symbol behaves as a tensor product of differentials of logarithms. Thus it also obeys the property

$$A \otimes c \otimes B = 0 \tag{5.13}$$

for any nonzero constant c, allowing us to discard terms of this form.

Furthermore, we need to extract the divergent logarithms in the variables ε_i. In general, the structure of the limit is such that, at loop order L, divergences of degree $\log^{L-1}$ appear. At two loops, we will thus have at most single logarithms, which come from symbols with

JHEP05(2016)012

one of the ε_i in one entry. We may extract the divergent logarithms by virtue of the shuffle identity

$$\varepsilon_i \otimes X \otimes Y = \log \varepsilon_i \, (X \otimes Y) - (X \otimes \varepsilon_i \otimes Y) - (X \otimes Y \otimes \varepsilon_i) \,, \tag{5.14}$$

which follows from writing $\log \varepsilon_i$ as an iterated integral and nesting its integration range with the $(X \otimes Y)$ integral it multiplies.

Finally, we have worked out the transformation (5.4), relating the multi-Regge variables w_i, $\bar{w}_i$ most commonly defined in terms of the cross ratios (4.3), (4.4), to a generalization of the variables used previously [9, 46]. Expanding once more the different factors in the symbol entries as in eq. (5.11), we observe the structure (5.1) up to $n = 10$ points, and conjecture it to hold for all multiplicities.

6 From symbols to functions

Of course it is of interest to lift the symbols $f, \tilde{f}$ and g to functions. For f and $\tilde{f}$ the answer is well-known even beyond the NLLA since the six gluon remainder function is known explicitly to very high loop order in multi-Regge kinematics [35, 37, 53], and implicitly also to all orders [4, 16]. For completeness, let us quote here the relevant two-loop result [8] in our conventions (5.2), where by slight abuse of notation f, $\tilde{f}$ now denote functions rather than symbols,[2]

$$\begin{aligned} f(w) &= \frac{1}{2} \log |1+w|^2 \log \frac{|1+w|^2}{|w|^2} \,, \\ \tilde{f}(w) &= -4\mathrm{Li}_3(-w) - 4\mathrm{Li}_3(-\bar{w}) + 2 \log |w|^2 (\mathrm{Li}_2(-w) + \mathrm{Li}_2(-\bar{w})) \\ &\quad + \frac{1}{3} \log^2 |1+w|^2 \log \frac{|w|^6}{|1+w|^4} - \frac{1}{2} \log |1+w|^2 \log \frac{|1+w|^2}{|w|^2} \log \frac{|w|^2}{|1+w|^4} \,, \end{aligned} \tag{6.1}$$

with $|w|^2 = w\bar{w}$ and $|1+w|^2 = (1+w)(1+\bar{w})$.

For the function associated to g, while it could in principle be obtained from the formula for the two-loop heptagon remainder function presented in [24], the latter is only valid in a subspace of the Euclidean region known as the positive region, thus rendering the analytic continuation relevant for the multi-Regge limit quite intricate.

Instead, in this section we will construct a prototype function whose symbol equals g by directly comparing it against a basis of functions having the same alphabet. That is, we first construct an ansatz for the function, which is a linear combination with undetermined coefficients, of all independent functions of transcendentality $m = 0, 1, 2, 3$, multiplied by transcendental constants such as $(i\pi)^k$ or (multiple) zeta values ζ_k, so that each term has uniform total transcendentality $m + k = 3$. Equating the symbol of the ansatz with g then fixes the coefficients of all terms with $m = 3$. We further reduce the ambiguity of the remaining terms with lower functional transcendentality by imposing simple constraints from symmetry, ending up with a prototype function with 25 undetermined parameters.

[2] Our expressions have an extra factor of 4 compared to [8] due to the use of $\lambda/(4\pi)^2$ as expansion parameter, as in [42]. In addition, here we have replaced the large logarithm by $\log(1-u_1) \to \frac{1}{2}\log\varepsilon_4 - \frac{1}{2}\log\frac{|w|^2}{|1+w|^4}$.

JHEP05(2016)012

We start by noting that a basis spanning the subset of 2dHPLs with the five-letter (unbarred) alphabet mentioned below (5.7) can be generated from

$$\mathcal{G} = \Big\{ G(\vec{a}; y) | a_i \in \{0, 1\} \Big\} \cup \Big\{ G(\vec{a}; x) | a_i \in \{0, 1, 1/y\} \Big\}, \tag{6.2}$$

where

$$G(a_1, \ldots, a_n; z) \equiv \begin{cases} \frac{1}{n!} \log^n z & \text{if } a_1 = \ldots = a_n = 0 \\ \int_0^z \frac{dt_1}{t_1 - a_1} G(a_2, \ldots, a_n; t_1) & \text{otherwise,} \end{cases} \tag{6.3}$$

with $G(; z) = 1$, are iterated integrals over a particular curve, known as Goncharov or multiple polylogarithms (MPLs). The basis (6.2) is in turn the part of the hexagon function basis considered in [54] (before imposing branch cut conditions) that is independent of one of the three so-called y-variables. From the recursive definition of the symbol of MPLs,

$$\begin{aligned} \mathrm{S}[G(a_{n-1}, \ldots, a_1; a_n)] = \sum_{i=1}^{n-1} \Big[& \mathrm{S}[G(a_{n-1}, \ldots, \hat{a}_i, \ldots, a_1; a_n)] \otimes (a_i - a_{i+1}) \\ & - \mathrm{S}[G(a_{n-1}, \ldots, \hat{a}_i, \ldots, a_1; a_n)] \otimes (a_i - a_{i-1}) \Big], \end{aligned} \tag{6.4}$$

where $a_0 = 0$ and hatted indices are omitted, it is straightforward to see that the 2dHPLs in eq. (6.2) indeed yield the five-letter alphabet mentioned below eq. (5.7).

In fact, allowing the entries of the singularity vector $\vec{a} \equiv (a_1, \ldots, a_n)$ to take any value within the prescribed set in the basis (6.2) yields an overcomplete system, because of shuffle identities such as

$$G(a; z)\, G(b; z) = G(a, b; z) + G(b, a; z), \tag{6.5}$$

which follow from the definition (6.3) by nesting the integration range of the integrals on the left-hand side. According to Radford's theorem [55], we may solve these identities and obtain a linearly independent set of functions by only keeping the singularity vectors that form Lyndon words. That is, if we consider all words made of letters of a given alphabet, the latter also defining a particular ordering between the letters, then Lyndon words are those words that no matter how we split them into two substrings, the left substring is always lexicographically smaller than the right substring.

For example, all Lyndon words up to length three of the alphabet $0 < 1 < 2$ are

$$0, \quad 1, \quad 2, \quad 01, \quad 02, \quad 12, \quad 001, \quad 002, \quad 011, \quad 012, \quad 021, \quad 022, \quad 112, \quad 122, \tag{6.6}$$

and from this example we may obtain all irreducible 2dHPLs of eq. (6.2) as follows:[3] replacing $2 \to 1/y$ yields the singularity vectors $\vec{a}$ of all irreducible 2dHPLs on the right hand side of eq. (6.2), and discarding all words with the letter 2 yields the respective ones on the left-hand side of the latter formula. Let us call the Lyndon basis of $G(\vec{a}; y), G(\vec{a}; x)$, with singularity vectors as obtained by the aforementioned two operations, as $\mathcal{G}^L \subset \mathcal{G}$.

So far we have constructed irreducible functions with only half of the ten-letter alphabet appearing in the symbol g. Clearly, functions for the other half of the alphabet may be

[3] Namely, those 2dHPLs which cannot be written as a product of lower-weight 2dHPLs.

JHEP05(2016)012

obtained by the complex conjugate of $\mathcal{G}^L$, $\overline{\mathcal{G}}^L$. Now it turns out that as a consequence of the local path independence of iterated integrals, also known as the integrability condition, and the fact that no letter mixes barred and unbarred variables (for example, we don't encounter letters of the form $1 + w\bar{w}$), there exist no other irreducible functions whose symbol entries span the entire ten-letter alphabet in question.

In summary, all irreducible functions with the same alphabet as g are given by $\mathcal{G}^L \cup \overline{\mathcal{G}}^L$, and to obtain a complete basis at a given weight, one needs to add to the latter all distinct products of lower-weight functions from the same set, and with the same total weight. In this manner, we obtain a basis of dimension 1, 10, 63, and 320 at weights 0 (i.e. $G[;z] = 1$), 1, 2, and 3, respectively. Forming a linear combination of functions at weight 3 with arbitrary coefficients, taking its symbol with the help of eq. (6.4) and equating the result with the symbol g, we uniquely determine the 320 coefficients. In particular, we find that (exceptionally, g here denotes the function rather than the symbol)

$$
\begin{aligned}
2g(-1/y,-x) = {} & G(1,x)G(1,y)G\left(0,\bar{x}\right) + G(1,x)G(1,y)G\left(0,\bar{y}\right) + G(0,x)G(1,y)G\left(1,\bar{x}\right) \\
& + G(0,y)G(1,y)G\left(1,\bar{x}\right) - 2G(1,x)G(1,y)G\left(1,\bar{x}\right) \\
& - G(1,y)G\left(0,\bar{y}\right)G\left(1/y,x\right) + G(0,y)G(1,y)G\left(1/\bar{y},\bar{x}\right) \\
& + G(0,x)G(1,x)G\left(1,\bar{y}\right) + G(1,x)G(0,y)G\left(1,\bar{y}\right) \\
& - G(1,x)G\left(0,\bar{x}\right)G\left(1/y,x\right) + G(0,x)G\left(1,\bar{x}\right)G\left(1/y,x\right) \\
& + G(0,y)G\left(1,\bar{y}\right)G\left(1/y,x\right) + G(0,x)G(1,x)G\left(1/\bar{y},\bar{x}\right) \\
& - 2G(0,1,x)G\left(1/\bar{y},\bar{x}\right) - 2G(0,1,y)G\left(1/\bar{y},\bar{x}\right) - 2G\left(1,\bar{x}\right)G\left(0,1/y,x\right) \\
& + 2G\left(1,\bar{x}\right)G\left(1,1/y,x\right) - 2G\left(1,\bar{y}\right)G\left(1,1/y,x\right) - 2G(0,x)G(1,x)G\left(1,\bar{x}\right) \\
& + 2G(0,1,x)G\left(0,\bar{x}\right) + 2G(0,1,x)G\left(1,\bar{x}\right) - 2G(0,y)G(1,y)G\left(1,\bar{y}\right) \\
& + 2G(0,1,y)G\left(0,\bar{y}\right) + 2G(0,1,y)G\left(1,\bar{y}\right) + G(0,x)G(1,x)G(1,y) \\
& + G(1,x)G(0,y)G(1,y) - G(0,y)G(1,y)G\left(1/y,x\right) - 2G(1,y)G\left(1,1/y,x\right) \\
& - G(0,x)G(1,x)G\left(1/y,x\right) + 2G(0,1,x)G\left(1/y,x\right) + 2G(0,1,y)G\left(1/y,x\right) \\
& + 2G(1,x)G\left(0,1/y,x\right) + 2G(1,x)G\left(1,1/y,x\right) - 4G\left(0,1,1/y,x\right) \\
& - 4G\left(0,1/y,1,x\right) - 4G\left(1,1,1/y,x\right) \\
& + 2G(0,x)G(0,1,x) - 2G(1,x)G(0,1,x) - 4G(0,0,1,x) + 4G(0,1,1,x) \\
& - 2G(0,1,y)G(1,y) + 2G(0,y)G(0,1,y) - 4G(0,0,1,y) + 4G(0,1,1,y) \\
& + (x \leftrightarrow \bar{x},\, y \leftrightarrow \bar{y}) + \text{lower-weight functions.}
\end{aligned}
\tag{6.7}
$$

In order to fix the function completely, we need to address the coefficients of the remaining lower-weight functions multiplying the independent transcendental constants $(i\pi), \zeta_2, (i\pi)^3$ and ζ_3, so that the total weight is 3, which thus sum up to 75.

We have explained before that this information on contributions of lower weight is invisible to the symbol. However we may further constrain these terms by examining the symmetries of the problem. MHV amplitudes are invariant under parity (spatial reflection), which in the multi-Regge limit amounts to the transformation $w_i \leftrightarrow \bar{w}_i$ [46]. Imposing this condition on our ansatz leaves 2, 5, and 34 undetermined parameters multiplying functions of weight 0, 1, and 2, respectively.

JHEP05(2016)012

Furthermore, we have target-projectile symmetry, corresponding to an invariance under exchange of the incoming momenta, or equivalently under $w_k \to 1/w_{n-4-k}$, see e.g. [27]. For $g(v_1, v_2)$ as defined in eqs. (5.3)–(5.4), and given that $f(v) = f(1/v)$ [46] and similarly for $\tilde{f}$, this amounts to symmetry under $v_1 \leftrightarrow 1/v_2$ (or $x \leftrightarrow y$), which further reduces the number of unknowns to 2, 3, and 20, by order of increasing functional transcendentality. The only additional subtlety when imposing this symmetry comes from mapping the transformed functions back into the basis. For all but one, this can be done immediately due to the following property of MPLs,

$$G(a_1, \ldots, a_k; z) = G(xa_1, \ldots, xa_k; xz)\,. \tag{6.8}$$

for $a_k \neq 0$ and $x \in \mathbb{C}^*$. And for the one left, we may use the identity

$$G(1, 1/x; y) = G(1; x)G(1, y) + G(0, 1/y; x) - G(1, 1/y; x)\,, \tag{6.9}$$

which follows from the quasi-shuffle algebra of MPLs, see for example [31].

This concludes the discussion on the use of symmetry in constraining the terms of lower functional transcendentality. The final result for the 25-parameter functional representative for g (also including the functions for $f, \tilde{f}$), or equivalently the two-loop seven-point remainder function in multi-Regge kinematics, is included in the MATHEMATICA file `gfunction.m` attached to this publication. It would be interesting to fix the function completely, by further exploiting its expected analytic properties [37], overlap with the collinear limit [16, 35], or better yet by constructing the seven-point remainder function with proper branch cuts in general kinematics, and taking its limit. We leave these exciting questions for future work.

7 Conclusions

Let us comment a bit more on the three main results of this paper. At the end of section 4 we found a set of relations that determine the multi-Regge limit of the symbol of all Mandelstam regions from the regions $I = [k, l]$ with adjacent flips. The argument we presented is actually not restricted to the two-loop remainder function; in fact, it can easily be seen that it extends to all loops. This does not imply, however, that the multi-Regge limit of the remainder function itself satisfies similar relations. While the relations hold for the terms of maximal functional transcendentality, they are well known to receive additional contributions from lower transcendentality, such as double cut contributions. It would be interesting to study these modifications in more detail.

Thereby, one should also be able to resolve the observed discrepancy between the weak and strong coupling results for $n = 7$ external gluons in the Mandelstam region $4, 6$ in which the signs are flipped for the outgoing particles in position 4 and 6. In this case, the multi-Regge limit of the remainder function was shown to be non-trivial at weak coupling, in full agreement with our analysis of the two loop symbol, while the continuation at strong coupling produced a vanishing result [27]. Our investigation of the symbol suggests that the issue is related to the choice of the curve along which the kinematic invariants are

JHEP05(2016)012

continued in the strongly coupled theory. The curve selected in [27] possesses the desired winding numbers around $u_{ij} = 0$ but does not seem to belong to the right homotopy class. This issue certainly deserves further attention.

The second outcome of our analysis concerns the building blocks f and g of the multi-Regge limit. We found that, in multi-Regge kinematics, the symbol of the two loop remainder function can be built from terms that are entirely determined from the expressions with $n = 6$ and $n = 7$ external gluons. This result is a consequence of the low loop order. Generalizing arguments that were presented in [9], one can show that the multi-Regge limit of the L-loop remainder function is determined by L different building blocks $g^{(\nu)}, \nu = 1, \ldots, L$. The first two of these are $g^{(1)} \equiv f$ and $g^{(2)} = g$. The remaining ones may be reconstructed from processes involving up to $n = L + 5$ external gluons. They receive their leading contribution at $\mathrm{N}^{\nu-1}\mathrm{LLA}$. In going to higher loop orders, the building blocks $g^{(\nu)}$ themselves pick up higher order terms from the expansion in large logarithms. For $g^{(1)} = f$, for example, our two loop analysis only allowed to determine LLA and NLLA terms. In order to find $g^{(1)}$ to $\mathrm{N}^2\mathrm{LLA}$ accuracy, we need to analyze the known three loop symbol for $n = 6$ external gluons.

Let us finally mention that our results also impose strong constraints on the production vertex that appears in the multi-Regge limit for $n = 7$ external gluons. In particular, by transforming the prototype function for g, we could fix this vertex in NLLA, up to 25 parameters. In LLA, the relevant production vertex was actually computed by Bartels et al. [26]. It would be interesting to reproduce their result from our expressions, and to extract its NLLA corrections. This could in turn be used as a seed in order to compute the $n = 7$ remainder function to NLLA in principle at any loop order from the BFKL formula of [26], thus providing potentially useful boundary data for the amplitude bootstrap program [11, 12, 25, 54, 56, 57]. More generally, the integrability of $\mathcal{N} = 4$ SYM theory raises the hope that all power-suppressed terms can be obtained to all loops also for any of points, similarly to the $n = 6$ case [16].

Acknowledgments

We wish to thank Jochen Bartels, Lance Dixon, James Drummond, Mark Spradlin, and Martin Sprenger for useful discussions and comments. The work of T.B. is supported by a Marie Curie International Outgoing Fellowship within the 7^{th} European Community Framework Programme under Grant No. PIOF-GA-2011-299865. The research leading to these results has received funding from the US Department of Energy under contract DE-AC02-76SF00515, the People Programme (Marie Curie Actions) of the European Union's Seventh Framework Programme FP7/2007-2013/ under REA Grant Agreement No. 317089 (GATIS), and from the SFB 676 "Particles, Strings and the Early Universe".

A Parametrization of the multi-Regge limit

We seek a good parametrization of the multi-Regge limit of (dual) conformally inequivalent null polygons. Natural variables for such polygons arose in the construction of the OPE for

JHEP05(2016)012

null polygon Wilson loops [5–7, 13, 49]. We will describe a slightly modified parametrization that features a canonical multi-Regge limit for any number of edges.

Just as for the Wilson loop OPE, we will start an arbitrary fixed reference null n-gon that we tessellate into a sequence of $(n-5)$ internal null tetragons and two boundary tetragons. Each null tetragon is stabilized by three conformal transformations. For each internal tetragon, we act with its stabilizing conformal transformations on all cusps of the polygon that lie "below" the internal tetragon. In this way, we generate a $3(n-5)$-dimensional family of conformally inequivalent null polygons. Our parametrization differs from the parametrization for the Wilson loop OPE [5–7, 13, 49] by the specific choice of tessellation, which in our case is tailored to the multi-Regge limit.

Momentum twistors. The two-loop symbol for MHV amplitudes [42] is expressed in terms of conformally invariant combinations of momentum twistors [58]. We therefore need a good parametrization of the n momentum twistors that parametrize the null n-gon (or n-point amplitude). Let us note some key properties of momentum twistors that will be relevant in the following. Points x in dual spacetime $\mathbb{R}^{1,3}$ are in one-to-one correspondence with null rays $X \in \mathbb{R}^{2,4}$, $X^2 = 0$, $tX \cong X$ [59]. When written as a bispinor, a null vector X decomposes into a pair of spinors, $X^{ab} = Z^{[a}\tilde{Z}^{b]}$. This is the usual map between spacetime points x and lines $(Z, \tilde{Z})$ in twistor space. Points x_i that are null separated translate to lines in twistor space that intersect and thus share a common spinor (twistor). A null polygon with n cusps x_i is hence parametrized by n momentum twistors Z_i, with $x_i \simeq (Z_i, Z_{i+1})$. Points that lie on a common null line in spacetime map to lines in twistor space that lie in a common plane and intersect in a common point. By definition, momentum twistors are $\mathrm{SO}(2,4)$ spinors, hence conformal transformations act on them via (right) multiplication by $\mathrm{SL}(4)$ matrices.

The hexagon. In a conformal theory, the simplest non-trivial null polygon is the hexagon. All null tetragons are conformally equivalent; the same is true for null pentagons. To parametrize an arbitrary fixed reference hexagon, pick six numerical momentum twistors $Z_{1,\dots,6}$. Each line (Z_i, Z_{i+1}) defines a cusp x_i of the hexagon. Now tessellate the hexagon by drawing the two (unique) null lines that connect the cusps x_4 and x_5 with the line x_{12}. These lines are characterized by points x_4^{int}, x_5^{int} on the line x_{12}, or equivalently by the momentum twistors Z_4^{int}, Z_5^{int} that mark the intersections of the lines (Z_4, Z_5) and (Z_5, Z_6) with the plane (Z_1, Z_2, Z_3), see figure 2. The cusps $(x_4, x_5, x_5^{\mathrm{int}}, x_4^{\mathrm{int}})$, or equivalently the momentum twistors $(Z_5, Z_5^{\mathrm{int}}, Z_2, Z_4^{\mathrm{int}})$ define the internal null tetragon. It is preserved by three conformal transformations [5]: one rotation in the plane orthogonal to the tetragon, parametrized by ϕ, and two non-compact conformal transformations parametrized by σ and τ that move points along the horizontal and vertical directions of the tetragon. In momentum-twistor space, these transformations are represented by an $\mathrm{SL}(4)$ matrix $M^{\mathrm{int}}(F, S, T)$ that depends on the three parameters $F = e^{i\phi}$, $S = e^{\sigma}$, $T = e^{-\tau}$. It must preserve the four momentum twistors of the internal tetragon, and hence is uniquely defined by its eigenvalues:

$$\big(Z_5, Z_2, Z_5^{\mathrm{int}}, Z_4^{\mathrm{int}}\big).M^{\mathrm{int}}(F,S,T) = \sqrt{F}\,\mathrm{diag}\big(1/FS, S/F, T, 1/T\big).\big(Z_5, Z_2, Z_5^{\mathrm{int}}, Z_4^{\mathrm{int}}\big)\,. \tag{A.1}$$

JHEP05(2016)012

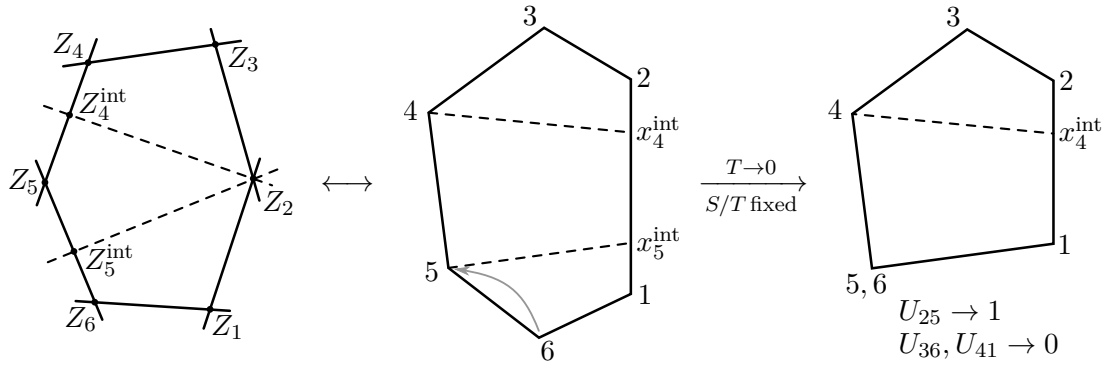

Figure 2. Illustration of the hexagon tessellation (center), its momentum-twistor picture (left), and the $2 \to 4$ Regge limit (center to right).

A family of conformally inequivalent null hexagons is now obtained by acting with the stabilizing matrix $M^{\text{int}}(F, S, T)$ of the internal tetragon on the momentum twistors Z_6, Z_1 that parametrize points "below" the internal tetragon.

The $2 \to 4$ multi-Regge limit of the hexagon is characterized by the following behavior of the three independent cross ratios:

$$U_{36} \to 0\,, \qquad U_{41}/U_{36} \qquad \text{and} \qquad (1-U_{25})/U_{36} \quad \text{finite}\,. \tag{A.2}$$

In our parametrization, this limit is attained for $T \to 0$ with S/T fixed,[4] which can be understood as follows: the limit $T \to 0$ "flattens" the bottom of the hexagon, while the simultaneous limit $S \to 0$ moves the bottom cusp x_6 towards x_5, see figure 2. It is then clear that U_{25} approaches 1, while x_{46} and x_{51} become lightlike, and therefore U_{36} and U_{41} go to zero (all at the same rate). In the limit, we find the following relations between the tessellation parameters F, S/T and the kinematic parameters w_4, $\bar{w}_4$ introduced in section 4:

$$F^2 = b\frac{\bar{w}_4}{w_4}\,, \qquad \frac{S^2}{T^2} = \frac{c}{w_4\bar{w}_4}\,. \tag{A.3}$$

Up to $\mathcal{O}(T^4)$, the three independent cross ratios then expand to

$$U_{25} = 1 - \frac{(1+w_4)(1+\bar{w}_4)}{w_4\bar{w}_4} a\,T^2\,, \qquad U_{36} = \frac{a\,T^2}{w_4\bar{w}_4}\,, \qquad U_{41} = a\,T^2\,. \tag{A.4}$$

The coefficients a, b, c are numerical constants whose values depend on the choice of reference hexagon. Below, we will give an explicit example for which $a = 1/4$, $b = 1$, $c = -1$.

General polygons. The parametrization of the hexagon straightforwardly generalizes to null polygons with any number of edges. Let $Z_{1,\ldots,n}$ be numerical momentum twistors that parametrize an arbitrary reference null n-gon. Tessellate the n-gon into $(n-5)$ internal tetragons and two boundary tetragons by drawing the (unique) null lines from cusps $x_4, \ldots, x_{n-1}$ to line x_{12}, see figure 3. These internal null lines are characterized by intersection points $x^{\text{int}}_{4,\ldots,n-1}$ on line x_{12}, or equivalently by the momentum twistors

[4] This is essentially the same limit as for the Wilson loop OPE parametrization [54, 60].

JHEP05(2016)012

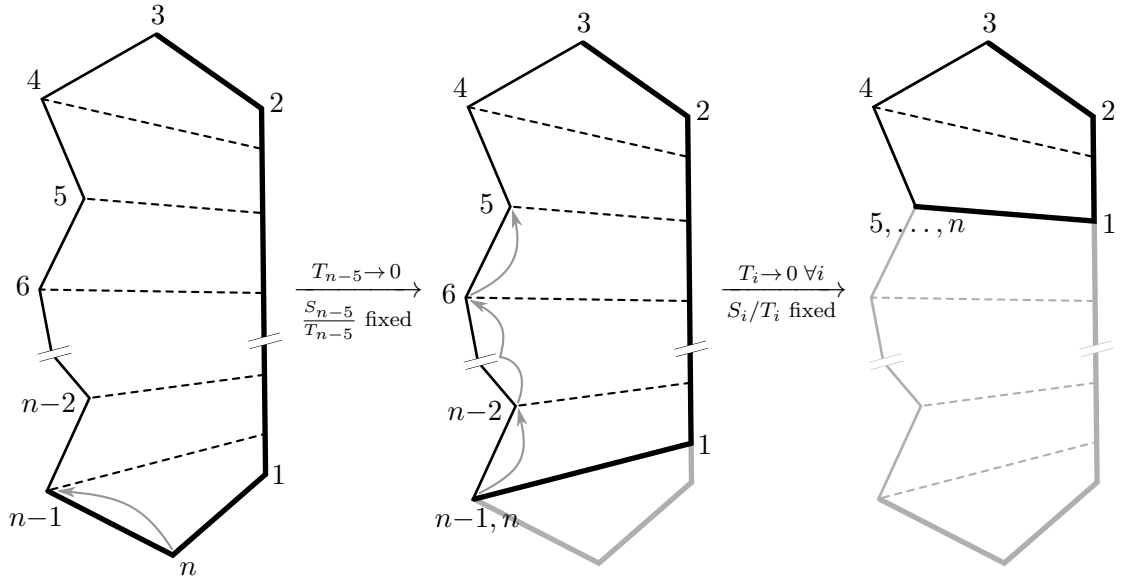

Figure 3. Tessellation of the null n-gon that is tailored to the $2 \to (n-2)$ multi-Regge limit (left), and systematics of the multi-Regge limit in the tessellation parameters (center and right). When $T_{n-5} \to 0$, S_{n-5}/T_{n-5} fixed (center), one can see that $U_{j,n-1} \to 1$ for $j = 2, \ldots, n-4$, and $U_{n-3,n}, U_{n-2,1} \to 0$. Similarly, $U_{i+2,n}, U_{i+3,1} \to 0$, $U_{j,i+4} \to 1$ for $j = 2, \ldots, i+1$ when $T_i \to 0$, S_i/T_i fixed. The right figure shows the full multi-Regge limit.

$Z^{\text{int}}_{4,\ldots,n-1}$ that mark the intersections of the twistor lines $(Z_4, Z_5), \ldots, (Z_{n-1}, Z_n)$ with the twistor plane (Z_1, Z_2, Z_3). Each internal tetragon is again stabilized by three conformal transformations parametrized by $F_j = e^{i\phi_j}$, $S_j = e^{\sigma_j}$, and $T_j = e^{-\tau_j}$, where $j = 1, \ldots, n-5$ enumerates the internal tetragons. In momentum-twistor space, these transformations are again realized by the unique SL(4) matrices M^{int}_j satisfying

$$\big(Z_{j+4}, Z_2, Z^{\text{int}}_{j+3}, Z^{\text{int}}_{j+4}\big).M^{\text{int}}_j = \sqrt{F_j}\,\text{diag}\big(1/F_jS_j, S_j/F_j, T_j, 1/T_j\big).\big(Z_{j+4}, Z_2, Z^{\text{int}}_{j+3}, Z^{\text{int}}_{j+4}\big)\,. \tag{A.5}$$

A family of conformally inequivalent null n-gons is now obtained by successively acting with the stabilizing matrices M^{int}_j, $j = n-5, \ldots, 1$ on the momentum twistors $Z_{j+5}, \ldots, Z_n, Z_1$ that parametrize cusps below the j'th internal tetragon.

In section 4, the $2 \to (n-2)$ multi-Regge limit was defined by $\varepsilon_j \to 0$, with $\tilde{u}_j$ and $(1-u_{j-2,j+1})^2/\varepsilon_j$ finite, for all $j = 4, \ldots, n-2$. This is equivalent to

$$U_{i+2,n} \to 0\,, \qquad U_{i+3,1}/U_{i+2,n} \quad \text{finite}\,, \qquad (1-U_{i+1,i+4})/U_{i+2,n} \quad \text{finite}\,. \tag{A.6}$$

In the above tessellation parameters, this limit is attained by $T_i \to 0$, S_i/T_i fixed, for all $i = 1, \ldots, n-5$. This can be understood in a similar fashion as for the hexagon, see figure 3: first, letting $T_{n-5} \to 0$, S_{n-5}/T_{n-5} fixed, takes $x_n \to x_{n-1}$, which means $U_{j,n-1} \to 1$ for $j = 2, \ldots, n-4$. At the same time, it implies that $x_{n-2,n}$ and $x_{n-1,1}$ become lightlike, which means $U_{n-3,n}$ and $U_{n-2,1}$ go to zero. Subsequently letting $T_{n-6} \to 0$, S_{n-6}/T_{n-6} fixed, takes $x_{n-1} \to x_{n-2}$, which implies $U_{j,n-2} \to 1$ for $j = 2, \ldots, n-5$, and $U_{n-4,n} \to 0$, $U_{n-3,1} \to 0$. This sequence continues: taking $T_i \to 0$, S_i/T_i fixed, implies $x_{i+5} \to x_{i+4}$,

JHEP05(2016)012

and thus $U_{i+2,n} \to 0$, $U_{i+3,1} \to 0$, and $U_{j,i+4} \to 1$ (all at the same rate) for $j = 2, \ldots, i+1$. Taking all $T_i \to 0$ with all S_i/T_i fixed completes the full multi-Regge limit. We find the following astonishingly simple relation between the tessellation parameters F_i, S_i/T_i and the multi-Regge kinematic variables w_i, $\bar{w}_i$ introduced in section 4:

$$F_i^2 = b_i \frac{\bar{w}_{i+3}}{w_{i+3}}\,, \qquad \frac{S_i^2}{T_i^2} = \frac{c_i}{w_{i+3}\,\bar{w}_{i+3}}\,. \tag{A.7}$$

Up to $\mathcal{O}(T_i^4)$, the large and small cross ratios expand to

$$U_{i+1,i+4} = 1 - \frac{(1+w_{i+3})(1+\bar{w}_{i+3})}{w_{i+3}\,\bar{w}_{i+3}}\,a_i\,T_i^2\,, \quad U_{i+2,n} = \frac{a_i\,T_i^2}{w_{i+3}\,\bar{w}_{i+3}}\,, \quad U_{i+3,1} = a_i\,T_i^2\,, \tag{A.8}$$

As for the hexagon, the coefficients a_i, b_i, and c_i are numerical constants whose values depend on the choice of reference n-gon. Experimentally, we find that one can always construct a reference n-gon such that $b_i = 1$, $c_i = -1$ for all $i = 1, \ldots, n-5$ in the above relations.

Explicit construction. The parametrization explained above can be based on arbitrary reference polygons (for example parametrized by n random momentum twistors). However, it is computationally very advantageous to start with numerically simple reference polygons. In the following, we outline how to construct such simple reference polygons. Explicit parametrizations for up to ten particles can be found in the MATHEMATICA file `mrlparam.m` attached to this publication.

Conformally inequivalent null hexagons can be parametrized as follows (cf. figure 2):

$$\begin{aligned} &Z_1 = (1,0,4,1).M_1\,, \quad Z_3 = (1,0,1,1)\,, \quad Z_5 = (0,1,0,0)\,, \quad Z_4^{\text{int}} = (0,0,0,1)\,, \\ &Z_2 = (1,0,0,0)\,, \quad Z_4 = (0,-1,0,1)\,, \quad Z_6 = (0,1,1,0).M_1\,, \quad Z_5^{\text{int}} = (0,0,1,0)\,, \end{aligned} \tag{A.9}$$

where M_1 stabilizes the internal tetragon $\{Z_5, Z_2, Z_4^{\text{int}}, Z_5^{\text{int}}\}$,

$$M_1(F,S,T) = \sqrt{F}\,\text{diag}\big(S/F, 1/(FS), 1/T, T\big)\,. \tag{A.10}$$

The reference hexagon (the above hexagon for $F = S = T = 1$) can be obtained from an arbitrary null hexagon by first picking a conformal frame in which $\{Z_2, Z_5, Z_4^{\text{int}}, Z_5^{\text{int}}\}$ take the above values, then applying a conformal transformation that preserves the internal triangle and that takes $\{Z_3, Z_4\}$ to the above values, and finally choosing an origin for the transformation M_1 such that $\{Z_6, Z_1\}$ take the above values. The $2 \to 4$ multi-Regge limit is attained by letting $T \to 0$ with S/T fixed. Setting

$$F = \frac{\sqrt{\bar{w}_4}}{\sqrt{w_4}}\,, \qquad \frac{S}{T} = -\frac{1}{\sqrt{w_4}\sqrt{\bar{w}_4}}\,, \tag{A.11}$$

the independent cross ratios up to $\mathcal{O}(T^4)$ expand to

$$U_{25} = 1 - \frac{(1+w_4)(1+\bar{w}_4)}{w_4\,\bar{w}_4}\,\frac{T^2}{4}\,, \qquad U_{36} = \frac{1}{w_4\,\bar{w}_4}\,\frac{T^2}{4}\,, \qquad U_{41} = \frac{T^2}{4}\,, \tag{A.12}$$

that is, (A.7), (A.8) is satisfied with $a_1 = 1/4$, $b_1 = 1$, $c_1 = -1$.

JHEP05(2016)012

A convenient parametrization of the null heptagon can be obtained by extending the above null hexagon such that the edge x_{61} of the hexagon becomes the internal null line from cusp x_6 to line x_{12} of the heptagon. That is, Z_1 of the hexagon becomes Z_6^{int} of the heptagon. To the configuration (A.9) one only needs to add a new momentum twistor Z_7 that lies on the line (Z_6, Z_6^{int}), and a new momentum twistor Z_1 that lies in the plane $(Z_6^{\text{int}}, Z_2, Z_3)$. This makes three new degrees of freedom, which can be mapped to the parameters F_2, S_2, T_2 of the new internal tetragon. A useful choice yields

$$\begin{aligned}
Z_1 &= (3,0,12,4).M_2.M_1\,, & Z_5 &= (0,1,0,0)\,, & Z_4^{\text{int}} &= (0,0,0,1)\,,\\
Z_2 &= (1,0,0,0)\,, & Z_6 &= (0,1,1,0).M_1\,, & Z_5^{\text{int}} &= (0,0,1,0)\,,\\
Z_3 &= (1,0,1,1)\,, & Z_7 &= (-1,4,0,-1).M_2.M_1\,, & Z_6^{\text{int}} &= (1,0,4,1).M_1\,,\\
Z_4 &= (0,-1,0,1)\,, & & & & \qquad (A.13)
\end{aligned}$$

where M_1 is the matrix (A.10), but with arguments F_1, S_1, T_1, and

$$M_2(F_2,S_2,T_2) = \sqrt{F_2}\begin{pmatrix} S_2/F_2 & 0 & 0 & 0\\ 0 & 1/(F_2S_2) & 1/(F_2S_2)-T_2 & 0\\ 0 & 0 & T_2 & 0\\ (F_2-S_2T_2)/(F_2T_2) & 0 & 4(1-T_2^2)/T_2 & 1/T_2 \end{pmatrix} \qquad (A.14)$$

stabilizes the new internal tetragon formed by $\{Z_6, Z_2, Z_5^{\text{int}}, Z_6^{\text{int}}\}\big|_{M_1=\text{id}}$ according to (A.5). As described above, the $2\to 5$ multi-Regge limit of the heptagon is obtained by letting $T_1, T_2 \to 0$ with S_1/T_1, S_2/T_2 fixed. Identifying

$$F_i = \frac{\sqrt{\bar w_{i+3}}}{\sqrt{w_{i+3}}}\,, \qquad \frac{S_i}{T_i} = -\frac{1}{\sqrt{w_{i+3}}\sqrt{\bar w_{i+3}}}\,, \qquad i=1,2 \qquad (A.15)$$

yields for the independent cross ratios up to $\mathcal{O}(T_i^4)$:

$$U_{25} = 1 - \frac{(1+w_4)(1+\bar w_4)}{w_4\,\bar w_4}\,\frac{T_1^2}{4}\,, \qquad U_{37} = \frac{1}{w_4\,\bar w_4}\,\frac{T_1^2}{4}\,, \qquad U_{41} = \frac{T_1^2}{4} \qquad (A.16)$$

$$U_{36} = 1 - \frac{(1+w_5)(1+\bar w_5)}{w_5\,\bar w_5}\,\frac{T_2^2}{4}\,, \qquad U_{47} = \frac{1}{w_5\,\bar w_5}\,\frac{T_2^2}{4}\,, \qquad U_{51} = \frac{T_2^2}{4}\,, \qquad (A.17)$$

that is, (A.7), (A.8) again is satisfied with $a_i = 1/4$, $b_i = 1$, $c_i = -1$.

Iterating this procedure, one can obtain convenient parametrizations of null polygons with any number of edges. In the MATHEMATICA file `mrlparam.m` attached to this publication, we provide explicit parametrizations for which the multi-Regge limit (A.8) is attained upon the identification (A.7) with $a_i = 1/4$, $b_i = 1$, $c_i = -1$, for up to ten particles.

JHEP05(2016)012

References

[1] J.M. Drummond, J. Henn, V.A. Smirnov and E. Sokatchev, *Magic identities for conformal four-point integrals*, *JHEP* **01** (2007) 064 [hep-th/0607160] [INSPIRE].

[2] J.M. Drummond, J. Henn, G.P. Korchemsky and E. Sokatchev, *Conformal Ward identities for Wilson loops and a test of the duality with gluon amplitudes*, *Nucl. Phys.* **B 826** (2010) 337 [arXiv:0712.1223] [INSPIRE].

[3] Z. Bern, L.J. Dixon and V.A. Smirnov, *Iteration of planar amplitudes in maximally supersymmetric Yang-Mills theory at three loops and beyond*, *Phys. Rev.* **D 72** (2005) 085001 [hep-th/0505205] [INSPIRE].

[4] B. Basso, A. Sever and P. Vieira, *Hexagonal Wilson Loops in Planar $\mathcal{N} = 4$ SYM Theory at Finite Coupling*, arXiv:1508.03045 [INSPIRE].

[5] L.F. Alday, D. Gaiotto, J.M. Maldacena, A. Sever and P. Vieira, *An Operator Product Expansion for Polygonal null Wilson Loops*, *JHEP* **04** (2011) 088 [arXiv:1006.2788] [INSPIRE].

[6] D. Gaiotto, J.M. Maldacena, A. Sever and P. Vieira, *Bootstrapping Null Polygon Wilson Loops*, *JHEP* **03** (2011) 092 [arXiv:1010.5009] [INSPIRE].

[7] D. Gaiotto, J.M. Maldacena, A. Sever and P. Vieira, *Pulling the straps of polygons*, *JHEP* **12** (2011) 011 [arXiv:1102.0062] [INSPIRE].

[8] L.N. Lipatov and A. Prygarin, *BFKL approach and six-particle MHV amplitude in $N = 4$ super Yang-Mills*, *Phys. Rev.* **D 83** (2011) 125001 [arXiv:1011.2673] [INSPIRE].

[9] J. Bartels, A. Kormilitzin, L.N. Lipatov and A. Prygarin, *BFKL approach and $2 \to 5$ maximally helicity violating amplitude in $\mathcal{N} = 4$ super-Yang-Mills theory*, *Phys. Rev.* **D 86** (2012) 065026 [arXiv:1112.6366] [INSPIRE].

[10] J. Bartels, L.N. Lipatov and A. Prygarin, *Collinear and Regge behavior of $2 \to 4$ MHV amplitude in $N = 4$ super Yang-Mills theory*, arXiv:1104.4709 [INSPIRE].

[11] L.J. Dixon, J.M. Drummond and J.M. Henn, *Bootstrapping the three-loop hexagon*, *JHEP* **11** (2011) 023 [arXiv:1108.4461] [INSPIRE].

[12] L.J. Dixon, J.M. Drummond, C. Duhr, M. von Hippel and J. Pennington, *Bootstrapping six-gluon scattering in planar $N = 4$ super-Yang-Mills theory*, in proceedings of the *Loops and Legs in Quantum Field Theory*, Weimar, Germany, April 27–May 02 2014, [PoS(LL2014)077] [arXiv:1407.4724] [INSPIRE].

[13] B. Basso, A. Sever and P. Vieira, *Spacetime and Flux Tube S-Matrices at Finite Coupling for $N = 4$ Supersymmetric Yang-Mills Theory*, *Phys. Rev. Lett.* **111** (2013) 091602 [arXiv:1303.1396] [INSPIRE].

[14] B. Basso, A. Sever and P. Vieira, *Space-time S-matrix and Flux tube S-matrix II. Extracting and Matching Data*, *JHEP* **01** (2014) 008 [arXiv:1306.2058] [INSPIRE].

[15] B. Basso, A. Sever and P. Vieira, *Collinear Limit of Scattering Amplitudes at Strong Coupling*, *Phys. Rev. Lett.* **113** (2014) 261604 [arXiv:1405.6350] [INSPIRE].

[16] B. Basso, S. Caron-Huot and A. Sever, *Adjoint BFKL at finite coupling: a short-cut from the collinear limit*, *JHEP* **01** (2015) 027 [arXiv:1407.3766] [INSPIRE].

[17] B. Basso, J. Caetano, L. Cordova, A. Sever and P. Vieira, *OPE for all Helicity Amplitudes II. Form Factors and Data analysis*, *JHEP* **12** (2015) 088 [arXiv:1508.02987] [INSPIRE].

JHEP05(2016)012

[18] L.F. Alday and J.M. Maldacena, *Gluon scattering amplitudes at strong coupling*, *JHEP* **06** (2007) 064 [arXiv:0705.0303] [INSPIRE].

[19] L.F. Alday, D. Gaiotto and J.M. Maldacena, *Thermodynamic Bubble Ansatz*, *JHEP* **09** (2011) 032 [arXiv:0911.4708] [INSPIRE].

[20] L.F. Alday, J.M. Maldacena, A. Sever and P. Vieira, *Y-system for Scattering Amplitudes*, *J. Phys.* **A 43** (2010) 485401 [arXiv:1002.2459] [INSPIRE].

[21] J. Bartels, J. Kotanski and V. Schomerus, *Excited Hexagon Wilson Loops for Strongly Coupled $N = 4$ SYM*, *JHEP* **01** (2011) 096 [arXiv:1009.3938] [INSPIRE].

[22] J. Bartels, J. Kotanski, V. Schomerus and M. Sprenger, *The Excited Hexagon Reloaded*, arXiv:1311.1512 [INSPIRE].

[23] J. Bartels, A. Kormilitzin and L. Lipatov, *Analytic structure of the $n = 7$ scattering amplitude in $\mathcal{N} = 4$ SYM theory in the multi-Regge kinematics: Conformal Regge pole contribution*, *Phys. Rev.* **D 89** (2014) 065002 [arXiv:1311.2061] [INSPIRE].

[24] J. Golden and M. Spradlin, *An analytic result for the two-loop seven-point MHV amplitude in $\mathcal{N} = 4$ SYM*, *JHEP* **08** (2014) 154 [arXiv:1406.2055] [INSPIRE].

[25] J.M. Drummond, G. Papathanasiou and M. Spradlin, *A Symbol of Uniqueness: The Cluster Bootstrap for the 3-Loop MHV Heptagon*, *JHEP* **03** (2015) 072 [arXiv:1412.3763] [INSPIRE].

[26] J. Bartels, A. Kormilitzin and L.N. Lipatov, *Analytic structure of the $n = 7$ scattering amplitude in $\mathcal{N} = 4$ theory in multi-Regge kinematics: Conformal Regge cut contribution*, *Phys. Rev.* **D 91** (2015) 045005 [arXiv:1411.2294] [INSPIRE].

[27] J. Bartels, V. Schomerus and M. Sprenger, *Heptagon Amplitude in the Multi-Regge Regime*, *JHEP* **10** (2014) 067 [arXiv:1405.3658] [INSPIRE].

[28] J. Bartels, L.N. Lipatov and A. Prygarin, *Integrable spin chains and scattering amplitudes*, *J. Phys.* **A 44** (2011) 454013 [arXiv:1104.0816] [INSPIRE].

[29] J. Bartels, V. Schomerus and M. Sprenger, *Multi-Regge Limit of the n-Gluon Bubble Ansatz*, *JHEP* **11** (2012) 145 [arXiv:1207.4204] [INSPIRE].

[30] A.B. Goncharov, *Multiple polylogarithms and mixed Tate motives*, math.AG/0103059 [INSPIRE].

[31] C. Duhr, *Mathematical aspects of scattering amplitudes*, in proceedings of the *Theoretical Advanced Study Institute in Elementary Particle Physics: Journeys Through the Precision Frontier: Amplitudes for Colliders. (TASI 2014)*, June 2–27 2014, Boulder, Colorado, [arXiv:1411.7538] [INSPIRE].

[32] N. Arkani-Hamed, J.L. Bourjaily, F. Cachazo, A B. Goncharov, A. Postnikov and J. Trnka, *Scattering Amplitudes and the Positive Grassmannian*, arXiv:1212.5605 [INSPIRE].

[33] G. Papathanasiou, *Hexagon Wilson Loop OPE and Harmonic Polylogarithms*, *JHEP* **11** (2013) 150 [arXiv:1310.5735] [INSPIRE].

[34] G. Papathanasiou, *Evaluating the six-point remainder function near the collinear limit*, in proceedings of the *49th Rencontres de Moriond on QCD and High Energy Interactions*, La Thuile, Italy, March 22–29 2014, pp. 293–296, [*Int. J. Mod. Phys.* **A 29** (2014) 1450154] [arXiv:1406.1123] [INSPIRE].

[35] J.M. Drummond and G. Papathanasiou, *Hexagon OPE Resummation and Multi-Regge Kinematics*, arXiv:1507.08982 [INSPIRE].

JHEP05(2016)012

[36] J. Golden, A.B. Goncharov, M. Spradlin, C. Vergu and A. Volovich, *Motivic Amplitudes and Cluster Coordinates*, *JHEP* **01** (2014) 091 [arXiv:1305.1617] [INSPIRE].

[37] L.J. Dixon, C. Duhr and J. Pennington, *Single-valued harmonic polylogarithms and the multi-Regge limit*, *JHEP* **10** (2012) 074 [arXiv:1207.0186] [INSPIRE].

[38] A. Bonini, D. Fioravanti, S. Piscaglia and M. Rossi, *Strong Wilson polygons from the lodge of free and bound mesons*, *JHEP* **04** (2016) 029 [arXiv:1511.05851] [INSPIRE].

[39] A.V. Belitsky, *Nonperturbative enhancement of superloop at strong coupling*, arXiv:1512.00555 [INSPIRE].

[40] J. Bartels, L.N. Lipatov and A. Sabio Vera, *BFKL Pomeron, Reggeized gluons and Bern-Dixon-Smirnov amplitudes*, *Phys. Rev.* **D 80** (2009) 045002 [arXiv:0802.2065] [INSPIRE].

[41] V. Del Duca, C. Duhr and E.W.N. Glover, *Iterated amplitudes in the high-energy limit*, *JHEP* **12** (2008) 097 [arXiv:0809.1822] [INSPIRE].

[42] S. Caron-Huot, *Superconformal symmetry and two-loop amplitudes in planar $N = 4$ super Yang-Mills*, *JHEP* **12** (2011) 066 [arXiv:1105.5606] [INSPIRE].

[43] A.B. Goncharov, *A simple construction of Grassmannian polylogarithms*, arXiv:0908.2238 [INSPIRE].

[44] A.B. Goncharov, M. Spradlin, C. Vergu and A. Volovich, *Classical Polylogarithms for Amplitudes and Wilson Loops*, *Phys. Rev. Lett.* **105** (2010) 151605 [arXiv:1006.5703] [INSPIRE].

[45] C. Duhr, H. Gangl and J.R. Rhodes, *From polygons and symbols to polylogarithmic functions*, *JHEP* **10** (2012) 075 [arXiv:1110.0458] [INSPIRE].

[46] A. Prygarin, M. Spradlin, C. Vergu and A. Volovich, *All Two-Loop MHV Amplitudes in Multi-Regge Kinematics From Applied Symbology*, *Phys. Rev.* **D 85** (2012) 085019 [arXiv:1112.6365] [INSPIRE].

[47] T. Gehrmann and E. Remiddi, *Two loop master integrals for $\gamma^* \to 3$ jets: The Planar topologies*, *Nucl. Phys.* **B 601** (2001) 248 [hep-ph/0008287] [INSPIRE].

[48] K.-T. Chen, *Iterated path integrals*, *Bull. Am. Math. Soc.* **83** (1977) 831 [INSPIRE].

[49] A. Sever and P. Vieira, *Multichannel Conformal Blocks for Polygon Wilson Loops*, *JHEP* **01** (2012) 070 [arXiv:1105.5748] [INSPIRE].

[50] S. Mandelstam, *Cuts in the Angular Momentum Plane. 2*, *Nuovo Cim.* **30** (1963) 1148 [INSPIRE].

[51] J.M. Drummond, G.P. Korchemsky and E. Sokatchev, *Conformal properties of four-gluon planar amplitudes and Wilson loops*, *Nucl. Phys.* **B 795** (2008) 385 [arXiv:0707.0243] [INSPIRE].

[52] A. Brandhuber, P. Heslop and G. Travaglini, *MHV amplitudes in $N = 4$ super Yang-Mills and Wilson loops*, *Nucl. Phys.* **B 794** (2008) 231 [arXiv:0707.1153] [INSPIRE].

[53] J. Broedel and M. Sprenger, *Six-point remainder function in multi-Regge-kinematics: an efficient approach in momentum space*, arXiv:1512.04963 [INSPIRE].

[54] L.J. Dixon, J.M. Drummond, M. von Hippel and J. Pennington, *Hexagon functions and the three-loop remainder function*, *JHEP* **12** (2013) 049 [arXiv:1308.2276] [INSPIRE].

JHEP05(2016)012

[55] D.E. Radford, *A natural ring basis for the shuffle algebra and an application to group schemes*, *J. Algebra* **58** (1979) 432.

[56] L.J. Dixon and M. von Hippel, *Bootstrapping an NMHV amplitude through three loops*, *JHEP* **10** (2014) 065 [arXiv:1408.1505] [INSPIRE].

[57] L.J. Dixon, M. von Hippel and A.J. McLeod, *The four-loop six-gluon NMHV ratio function*, *JHEP* **01** (2016) 053 [arXiv:1509.08127] [INSPIRE].

[58] A. Hodges, *Eliminating spurious poles from gauge-theoretic amplitudes*, *JHEP* **05** (2013) 135 [arXiv:0905.1473] [INSPIRE].

[59] P.A.M. Dirac, *A Remarkable representation of the* $3+2$ *de Sitter group*, *J. Math. Phys.* **4** (1963) 901 [INSPIRE].

[60] Y. Hatsuda, *Wilson loop OPE, analytic continuation and multi-Regge limit*, *JHEP* **10** (2014) 038 [arXiv:1404.6506] [INSPIRE].

JHEP05(2016)012